Isotopic Yields of Fission Fragments produced in Multi-Nucleon Transfer-Induced Fission of ^{238}U in Inverse Kinematics

M. Caamaño,* F. Rejmund, X. Derkx, K.-H. Schmidt, M. Rejmund,
C. Golabek, A. Lemasson, A. Navin, T. Roger, and C. Schmitt
GANIL, CEA/DSM-CNRS/IN2P3, BP 55027, F-14076 Caen cedex 5, France

L. Andouin and C.-O. Bacri
IPN Orsay, IN2P3/CNRS-UPS, Georges Clemenceau 15 91406 Orsay, France

G. Barreau and B. Jurado
CENBG, IN2P3/CNRS-UB1, 33175 Gradignan cedex, France

J. Benlliure and E. Casarejos
Universidade de Santiago de Compostela, E-15706 Santiago de Compostela, Spain

B. Fernández Domínguez
University of Liverpool, Liverpool L69 7ZE, United Kingdom

L. Gaudefroy and J. Taieb
CEA/DAM Île-de-France, BP 12 91680 Bruyères-le-Châtel, France
(Dated: February 23, 2009)

A recent experiment at GANIL was performed to investigate the main properties of fission-fragments yields and energy distributions in different fissioning nuclei as a function of the excitation energy. Transfer reactions between a ^{238}U beam and a ^{12}C target produced different fissioning systems over a broad range of excitation energy below 30 MeV. The resulting actinides and their energy were determined from the reconstruction of the transfer reaction with the identification of the target-like recoil. The large acceptance spectrometer VAMOS was used to identify, in mass and charge, the fission fragments in-flight. As a result, the characteristics of the fission-fragment isotopic distributions of a variety of neutron-rich actinides are observed for the first time over the complete range of fission fragments.

PACS numbers:

I. INTRODUCTION

Fission produces the largest collective motion of nucleons inside the nuclei, while, at the same time, is also strongly influenced by the structure of the fissioning nucleus. At low excitation energy, shell structure and pairing correlations sign the main features of the fragment distribution.

It is well known that the fission fragment mass distribution of actinides in the range of masses from 230 to 256 are characterized by two or even three-humped shapes. This feature has been understood as superposition of independent fission modes [1, 2] corresponding to different paths in the potential surface of the fission process [2, 3]. The position of the heavy fragment was observed to remain constant around $M \sim 138$ in spontaneous and neutron-induced fission [3]. Similarly, campaigns of fusion-fission experiments showed a constant heavy-fragment mass at $M \sim 132$ and $M \sim 140$ [4]. These experimental results are well described with a symmetric and two asymmetric fission channels, being the asymmetric modes commonly associated with spherical and deformed neutron shells in $N = 82$ and $N \sim 84 - 90$ [4]. Recently, the study of fragment charge distribution in low-energy fission of neutron-deficient actinides showed an almost constant charge of the heavy fragment at $Z = 54$ [5]. This result is somehow surprising when compared with the neutron-shell influence described above, where a change of the average charge of the heavy fragment with the mass of the fissioning system was expected.

The controversy between the independent mass and charge measurements puts a strong constraint on the theoretical description of fission, and namely on what drives the process. The existence of systematic measurements of fission characteristics over a broad range of fissioning systems is very important to constraint the different models. Nonetheless, as different quantities were measured in the different sets of data (fission fragment mass in direct kinematics or charge in the case of inverse kinematics experiments), the simultaneous measurement of both mass and charge of fragments is imperatively required to go further. Information on full isotopic fragment distributions is very scarce; it mainly consists of

---
*Electronic address: caamano@ganil.fr

thermal neutron-induced fission of a few actinides [6–8], and restricted to the light fragment, due to technical difficulties in identifying high-Z products in direct kinematics. The isotopic distribution of the heaviest fragment may be determined using parallel radio-chemical techniques [9, 10], but with poor precision and in a reduced range of the total production. Another important characteristic of low energy fission in even-Z nuclei is the enhanced production of fragments with an even number of protons. This has been interpreted as a signature that completely paired proton configurations are preserved up to the scission point. The difference between production of even and odd charges may be related with the heating of the nucleus undergoing fission on its way to the scission point, and hence about the viscosity of the cold nuclear matter. Experimentally, the even-odd staggering has been observed to depend strongly on the fissility of the fissioning nucleus, as well as to vary with the charge split asymmetry [8].

The points discussed above indicate that a deeper insight into fission dynamics can only be gained with a systematic measurement of complete mass and charge distributions of fission fragments. This was the aim of the experiment performed in April 2008, based on multi-nucleon transfer-induced fission in inverse kinematics with the VAMOS spectrometer [11] at GANIL.

II. MULTI-NUCLEON TRANSFER-INDUCED FISSION OF ^{238}U IN INVERSE KINEMATICS

The experiment aimed to produce different fissioning system by multi-nucleon transfer reactions between a 6.15 MeV/u ^{238}U beam and a 20 mg/cm^2 ^{12}C target. The energy of the beam was chosen as a compromise between the fission cross-section and the tolerance of the detection system, mainly ruled by the damage on the Si detectors. At this energy, around 10% over the Coulomb barrier, we may expect a total fission cross-section between 0.1-1 barn, with a transfer-fission probability ten times lower [12].

Different fissioning systems are produced from the interaction of the U beam and the carbon target. Inelastic collisions provide a range of excitation energy to the ^{238}U beam, while transfer reactions produced a collection of fissile actinides, also in a range of excitation energy below 30 MeV. In addition, fusion-fission reactions produce fissile ^{250}Cf of 24 MeV of excitation energy, with a probability almost ten times larger than that of transfer-fission. The fission fragments produced will cover a wide range of energy (2-10 MeV/u), mass (90-150), atomic number (30-60), and charge states ($\sim$10 charges per isotope). Inverse kinematics of in-flight fission at 6 MeV/u confines the angular distribution of the fragments in a cone of about 25 deg in laboratory frame (see Fig. 1).
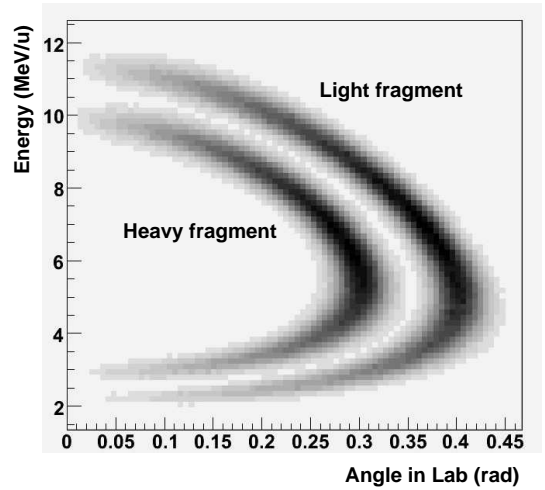

FIG. 1: Laboratory kinematics of typical fission fragments. Energy and angle data are simulated for a $Z = 54$, $M = 175$ heavy fragment, and a $Z = 38$, $M = 123$ light fragment

A. Experimental set-up

The kinematics reconstruction of the direct reactions where the fissioning systems are produced (inelastic scattering, multi-nucleon transfer) allows their identification, along with an estimation of their excitation energy. On the other hand, the characteristics of in-flight fission in inverse kinematics make it easier the detection of the most of the fragment distribution. These tasks are performed by two dedicated detection systems: the dE-E SPIDER telescope, and the VAMOS spectrometer.

SPIDER (Silicon Particle Identification DEtector in Ring) consists in two annular silicon detectors (see Fig. 2). Both are 48 mm radius double-faced detectors segmented into 1.5 mm 16 rings and 16 sectors, with an inner hole of 24 mm radius. The first detector, for measuring energy loss (dE), is 65 μm thick, while the second one, for residual energy (E_{res}), is 1 mm thick. The two detectors are placed 36 mm after the target, with a separation of 4 mm between them. The SPIDER ensemble is aimed to detect and identify the target-like recoil, by means of dE-E correlation (being E=dE+E_{res}), and to reconstruct the kinematics of direct reactions. This reconstruction is done with the total energy measurement and the determination of the recoil angle. The segmentation of the detectors allows a discrimination of $\sim$1 deg in the recoil angle; depending on the reaction, this is translated in $\sim$2 MeV of excitation energy resolution in both the recoil and the fissioning system. Figure 3 shows the dE-E correlation that allows to identify the different recoil species. Recoil identification resulted, at this stage of the analysis, in the detection of C, B, Be, Li and He isotopes; these correspond to U, Np, Pu, Am and Cm fissioning systems. So far, isotopic identification and determination of the excitation energy of the fissioning system are still under development. In addition, fusion-fission reactions
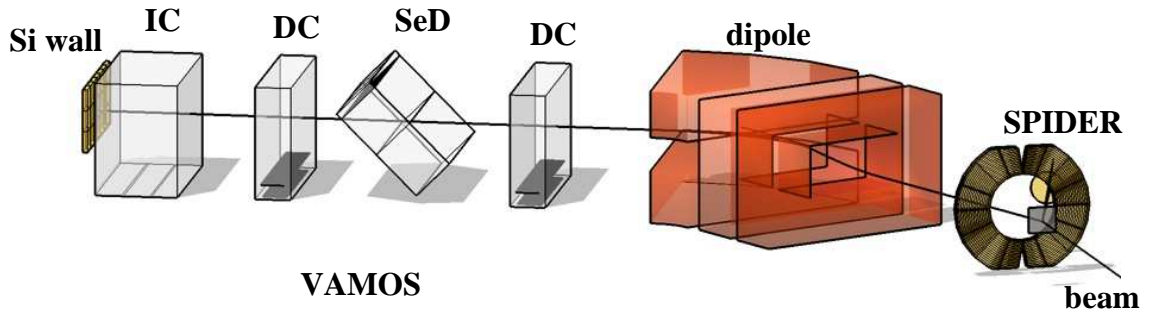
FIG. 2: Experimental Setup. The VAMOS spectrometer and associated detectors are depicted in the figure. The dE-E telescope SPIDER is placed between the target (in grey) and the magnets of the spectrometer (in red)

are also identified by the absence of target-like recoil, corrected by the SPIDER detector acceptance (around 4 srad).

Fission fragments produced passed through the inner hole of SPIDER, and they are identified in the VAMOS spectrometer and associated detectors (see Fig. 2). The whole spectrometer can be rotate around the target to cover an specific angular region. In this case, VAMOS was rotated 20 deg in order to cover the angular region with largest fragment production, close to the edge of the fission cone (see Fig. 1). This configuration allows the detection of one of the two fragments per fission. The geometry of VAMOS has an approximate angular acceptance of 14 deg in the horizontal plane, and ~3 deg in the vertical plane; the detection area accepts particles within 10 % of the central magnetic rigidity. In order to cover the most of the momentum and charge state distribution, different values of the central magnetic rigidity were used during the experiment.

The detection area in VAMOS was populated with two Drift Chambers (DC) to measure particle positions and angles, a Secondary Electron Detector (SeD) to measure the time of flight, an Ionization Chamber (IC) to measure energy loss, and a wall of twenty-one Silicon detectors to measure the residual energy of the particle. In addition, part of the Germanium-array gamma-detector EXOGAM [13] was placed around the target to collect gamma emission from the fission fragments.

B. Isotopic identification of fission fragment distributions

The information obtained by the detectors in VAMOS allows a complete identification of the fission fragments; that is, mass M, atomic number Z, charge state Q, and kinetic energy KE. In addition, the geometrical reconstruction gives angular information of the fragment at the target level (before entering VAMOS).

The total energy of the particle is the sum of the energy loss in the IC and the residual energy measured in the Si wall. The relation dE-E allows to separate the different Z detected in VAMOS, as we see in both panels of Fig. 4. Close to thirty different species, over a range of more than 600 MeV, are observed. At low energy, the shape of the lines is clearly different due to the Bragg peak corresponding to those particles stopping in the IC. The lines of Fig. 4 are an approach to described analytically the dE-E behaviour. In this approach, the energy loss dE depends on the velocity of the particle, and on an effective charge. The latter, depends also on the velocity, and on the Z of the particle. Corrections due to electron shell closing are also taken into account. This analytical description allows to assign a Z to individual events, with a resolution of $\Delta Z/Z \approx 1.5 \cdot 10^{-2}$ so far.

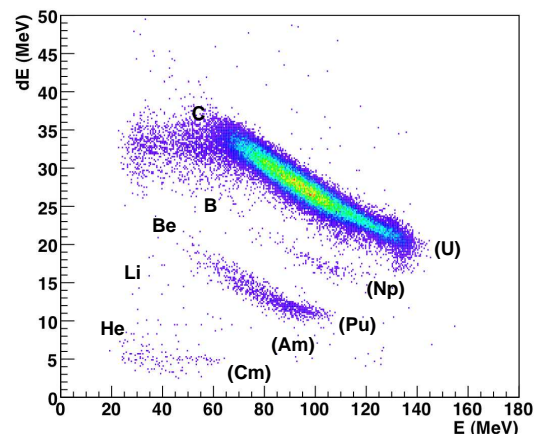The horizontal and vertical positions obtained in the

FIG. 3: Target-like recoil identification in SPIDER. Correlation between dE-E shows the different recoil species produced in inelastic and transfer reactions. The corresponding fissioning systems are indicated in parenthesis.
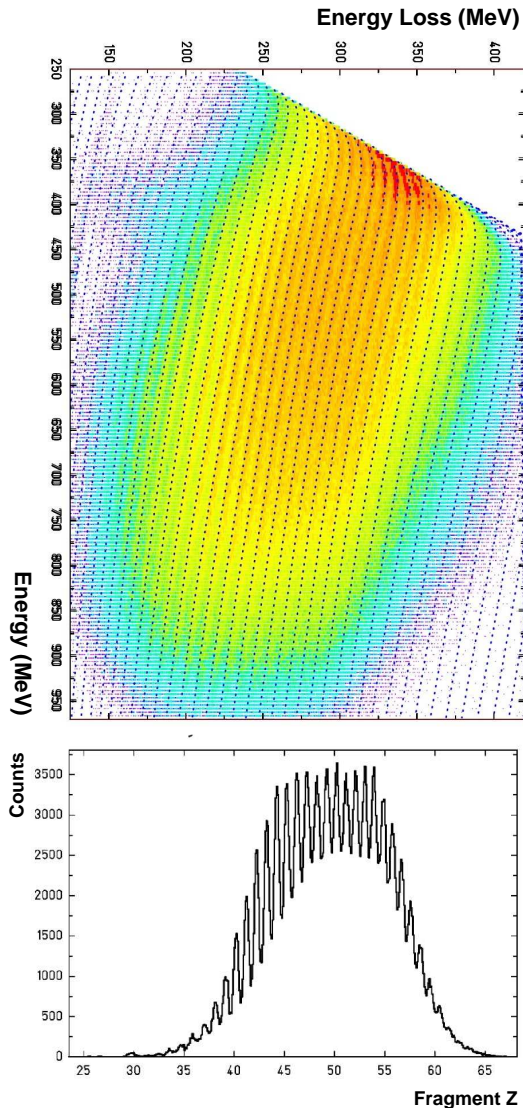
FIG. 4: Fragment Z identification in VAMOS. Upper panel: dE-E correlation. The lines correspond to the analytical description of dE-E correlation for each Z. Lower panel: Z projection along the analytical lines. The shape of the distribution is due to the addition of different sets of data not yet normalized.

two DC are used to determine the total path from the target, magnetic rigidity ($B\rho$), and angles at the target level. This is done by mapping of all possible trajectories before and after magnetic focusing (more details in [14, 15]). The time of flight, calculated between the SeD and the high frequency of the cyclotron, is combined with the reconstructed path to obtain the velocity. The mass of the fragments is calculated, in a first iteration, with the total energy and the velocity. The reconstructed Brho and the velocity are used to calculate the ratio M/Q. Figure 5 shows the relation M vs. M/Q, where the different mass-charge systems can be identified. The M identification is done in a second iteration that takes profit from the better resolution in M/Q: systems with the same Q
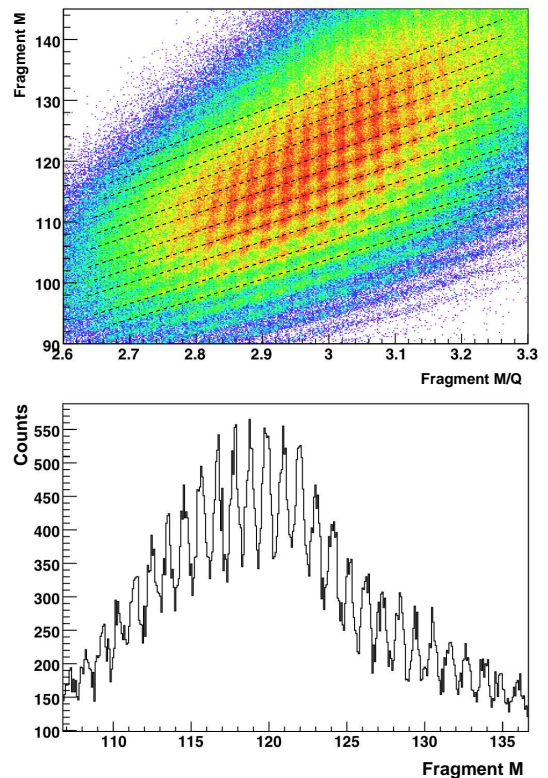

FIG. 5: Fragment M identification in VAMOS. Upper panel: M-M/Q correlation. The lines connect M-M/Q systems with the same charge state Q. Lower panel: M distribution of a single Q. The distribution is obtained with $M = M/Q \cdot Q$. The shape of the distribution is due to the addition of different sets of data not yet normalized.

form the diagonal lines in the M vs. M/Q relation. The final M identification is obtained multiplying the M/Q of systems contained in the same diagonal by the corresponding Q. This procedure allows the identification of more than 50 masses, from $M \approx 90$ to 140, with a resolution of $\Delta M/M \approx 0.6 \cdot 10^{-2}$ (see Fig. 5).

In addition, the set of EXOGAM gamma-detectors were used to identify gamma transitions in some of the fission fragments. The correlation between the gamma identification in some of the systems, and the Z and M obtained in the spectrometer allows an unambiguous identification of Z, M and Q of all fragments detected in VAMOS.

III. CONCLUSIONS AND PERSPECTIVES

The data analysis of the experiment is currently in its first stages, however some important achievements can already be highlighted. The multi-nucleon transfer between ^{238}U and ^{12}C produced a range of fissioning systems between U and Cm, already identified by dE-E correlation. In addition, fusion-fission reactions allowed to include ^{250}Cf in the collection of fissioning systems.

The measurement of fission fragments in inverse kinematics in the VAMOS spectrometer allowed, for the first time in a single experiment, the complete characterization of the whole distribution of fission fragments. More than 200 isotopes are identified in M, Z, and Q. The kinematic properties of the fragments are also determined by measuring KE and angle of fragments. These results show already the validity of this experimental approach, resulting in the most complete experimental characterization of fission in minor actinides so far.

In the next steps of the analysis, the kinematics reconstruction of the inelastic and transfer reactions with the SPIDER detector will allow the isotopic identification and the estimation of the excitation energy in the fissioning system. The identification of the whole fission fragment distribution, will be used to measure the frag-

ment yields and determined the characteristics of fragment production and energy distributions. For the first time, correlations between M and Z distributions will be possible, revealing shell effects,and the possible proton or neutron influence in the fission process. Also, the even-odd staggering in number of protons and neutrons can be explored in the whole fragment distribution.

Finally, the features of the fragment distribution are to be explored as a function of the entrance channel, this is, the fissioning system and its excitation energy. The fission cross section will be calculated with respect to the transfer probability, and in a more detailed analysis, the probability of fission will be determined for each system as a function of the excitation energy, giving information about the fission barrier.

[1] A. Turkevich et al., Phys. Rev. **84**, 52 (1951).
[2] A. Brosa et al., Phys. Rep. **197**, 167 (1990).
[3] K. F. Flynn et al., Phys. Rev. C **5**, 1725 (1972).
[4] M. G. Itkis et al., in *Dynamics at the Extreme 2000, Dubna* (2000).
[5] K.-H. Schmidt et al., Nucl. Phys. A **665**, 221 (2001).
[6] U. Quade et al., Nucl. Phys. A **487**, 1 (1988).
[7] J. L. Sida et al., Nucl. Phys. A **487**, 1 (1989).
[8] W. Lang et al., Nucl. Phys. A **345**, 34 (1989).
[9] I. Nishinaka et al., Phys. Rev. C **891**, 56 (1997).
[10] R. Tripathi et al., Phys. Rev. C **69**, 024613 (2004).
[11] H. Savajols et al., Nucl. Inst. and Meth. B **204**, 146 (2003).
[12] D. C. Biswas et al., Phys. Rev. C **56**, 1926 (1997).
[13] F. Azaiez, Nucl. Phys. A **654**, 1003c (1999).
[14] S. Pullanhiotan et al., Nucl. Inst. and Meth. A **593**, 343 (2008).
[15] S. Pullanhiotan et al., Nucl. Inst. and Meth. B **266**, 4148 (2008).